GSA DATA REPOSITORY 2015254

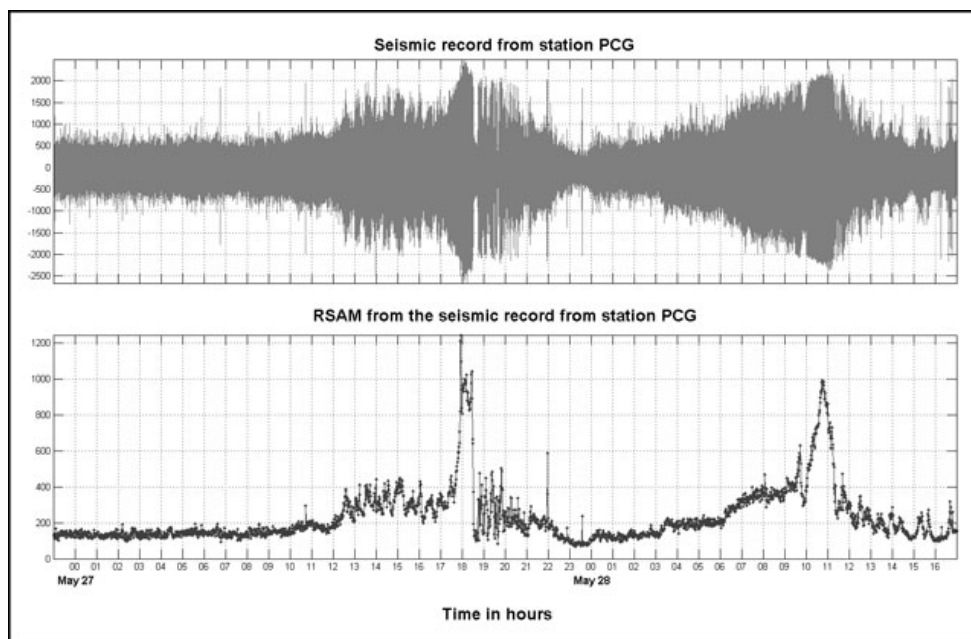**Supplementary Figures & Captions (DR1-DR7)**

Figure DR1. Seismicity recorded at Pacaya during the 2300 hour of May 26 through the 1700 hour on May 28 (local times). The upper panel shows the seismic record and the lower panel shows the computed RSAM. Station PCG is a short-period seismometer located on Cerro Chino, ~1 km northwest of Pacaya's summit on the MacKenney cone. Thermal IR GOES images of ash clouds on May 27 (https://www.youtube.com/watch?v=o-Vlpd7DuyQ) and May 28 (https://www.youtube.com/watch?v=LzElEznDMZk) show that plumes match the point of RSAM peaks on these dates. Seismic plot courtesy of INSIVUMEH and R. Escobar Wolf.
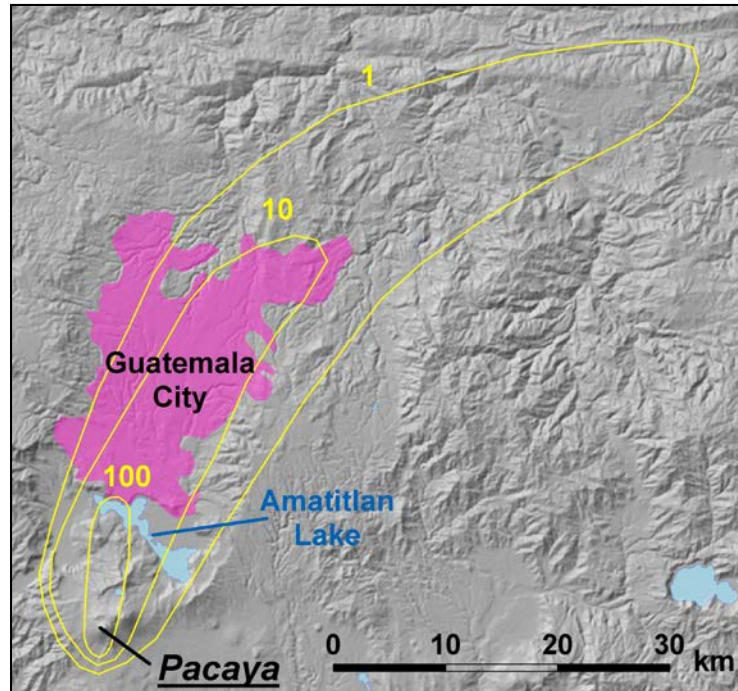
Figure DR2. Isopach maps modeled for the May 27, 2010 tephra eruption based on data published by SERVIR-CATHALAC. The values of the isopachs (in yellow) are given in millimeters. Populated centers (in pink), as well as the lakes (in blue) are also shown. Map modified from: Matías Gómez et al. (2012).
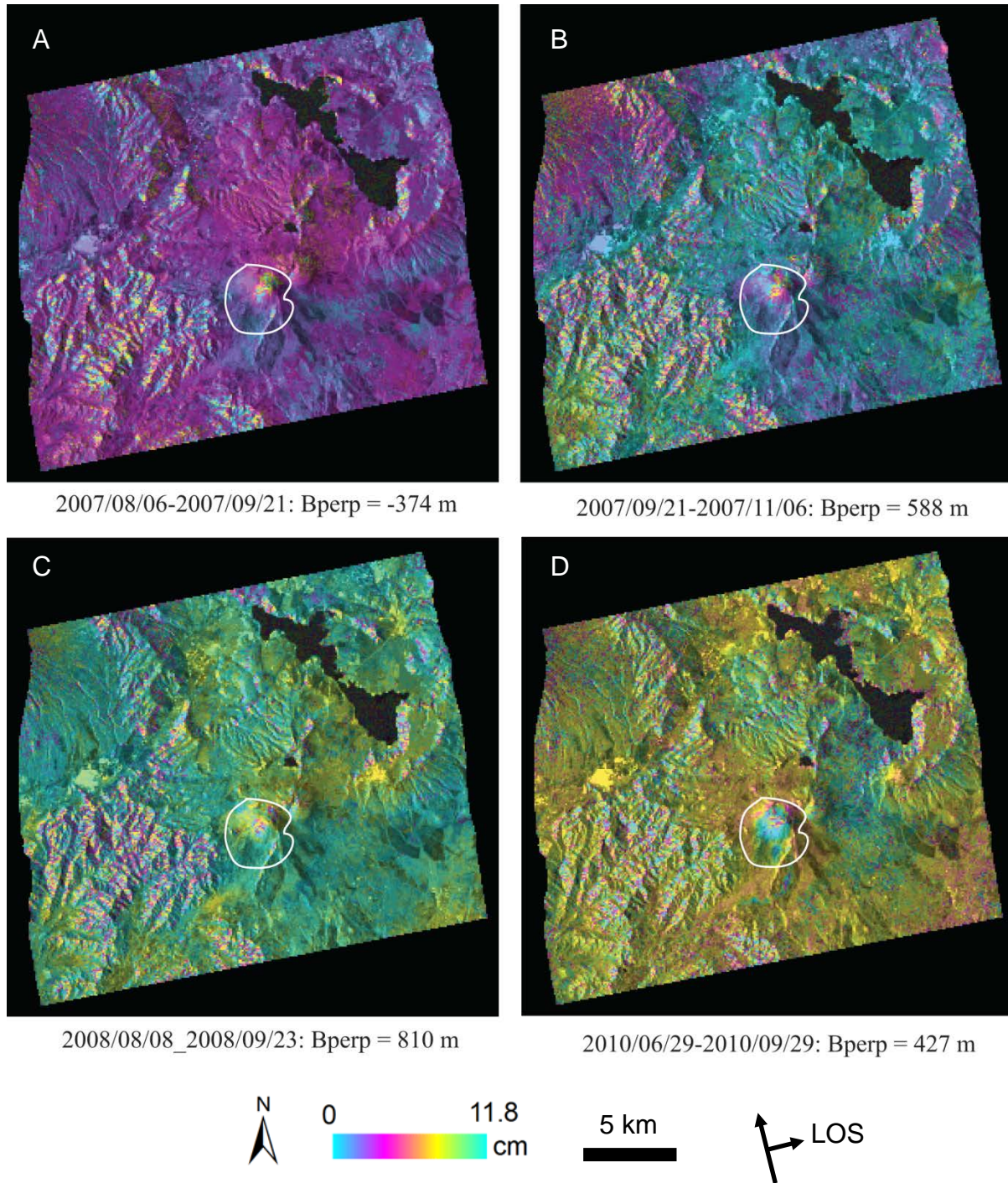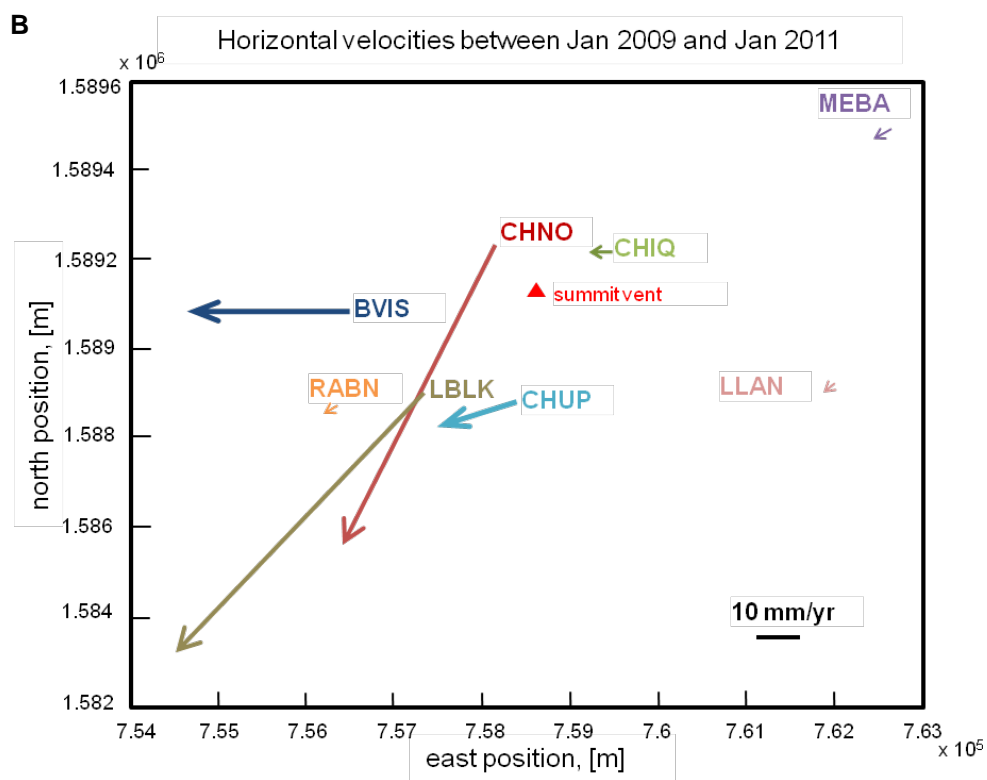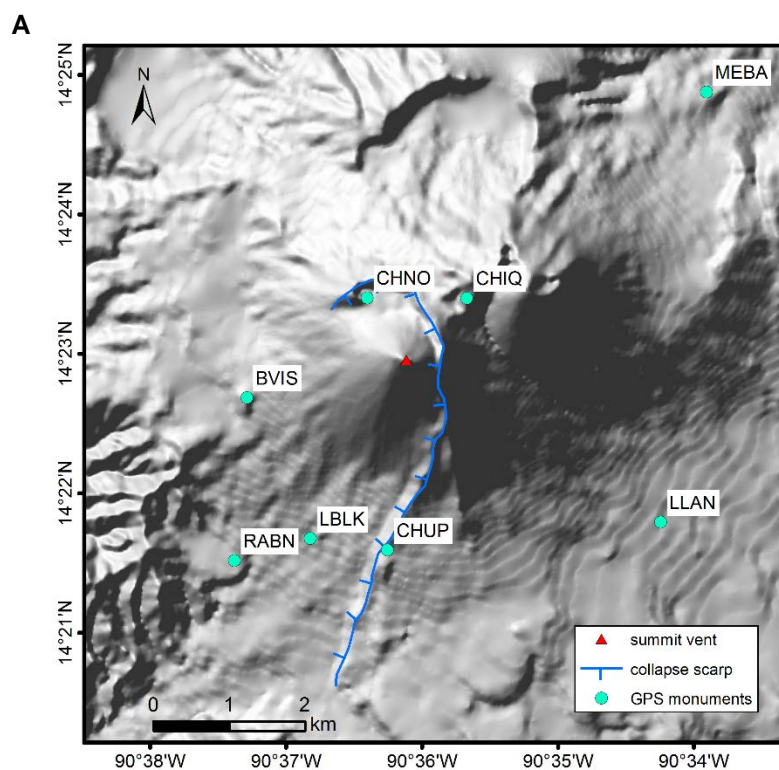
A 2007/08/06-2007/09/21: Bperp = -374 m

B 2007/09/21-2007/11/06: Bperp = 588 m

C 2008/08/08_2008/09/23: Bperp = 810 m

D 2010/06/29-2010/09/29: Bperp = 427 m

N

0   11.8
         cm

5 km

LOS

Figure DR3. (A-D) ALOS interferograms with large perpendicular baselines (374 – 810 m) do not show the fringes observed in the ALOS interferogram that spans the eruption, which has a perpendicular baseline of 369 m (Fig. 2A). Therefore, we can exclude DEM height errors as the cause of this deformation signal. The white line circles the extent of deformation observed from the interferograms in Fig. 2.
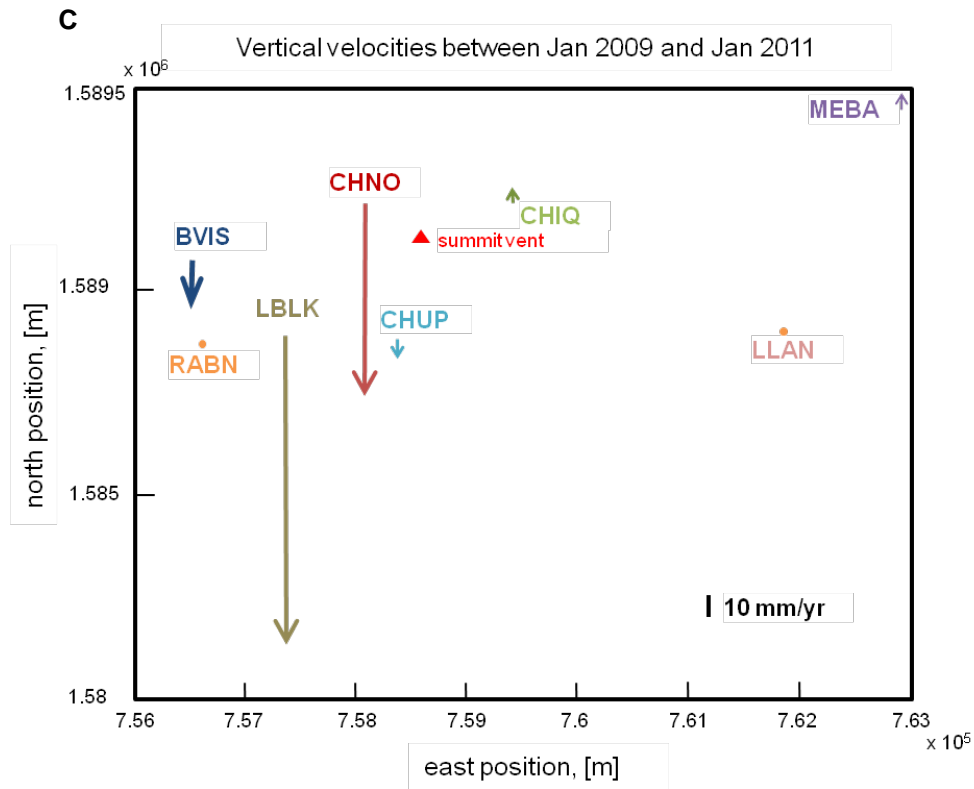
A

MEBA
CHNO   CHIQ
BVIS
RABN   LBLK   CHUP
LLAN

▲ summit vent
— collapse scarp
● GPS monuments

0   1   2
km

B

Horizontal velocities between Jan 2009 and Jan 2011

MEBA

CHNO ← CHIQ
▲ summit vent
← BVIS

RABN LBLK ← CHUP   LLAN

10 mm/yr

north position, [m]

east position, [m]

Figure DR4. (A) GPS locations around Pacaya. (B) Horizontal and (C) vertical GPS velocities measured between January 2009 and January 2011 at Pacaya. GPS station LBLK measured 0.53 m of downward and west to south-westward movement during this time. Station CHNO shows that similar movement occurred near the summit, an area where interferogram measurements are lost due to incoherence. Fig. DR5B and DR5C modified from: Hetland (2014).
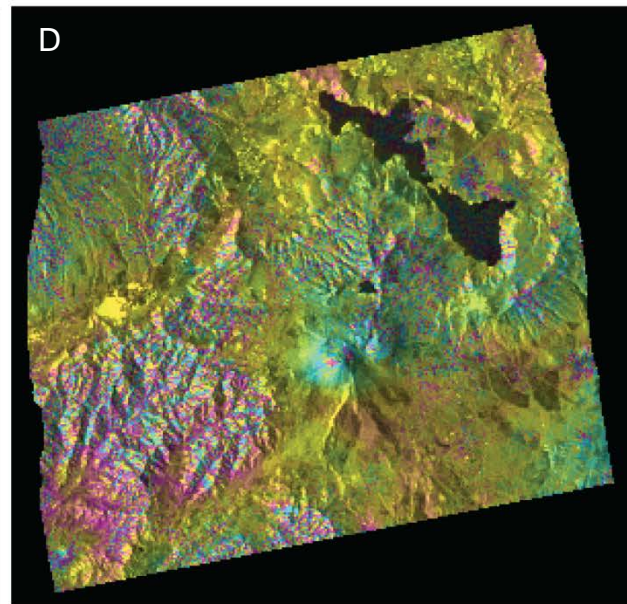
A
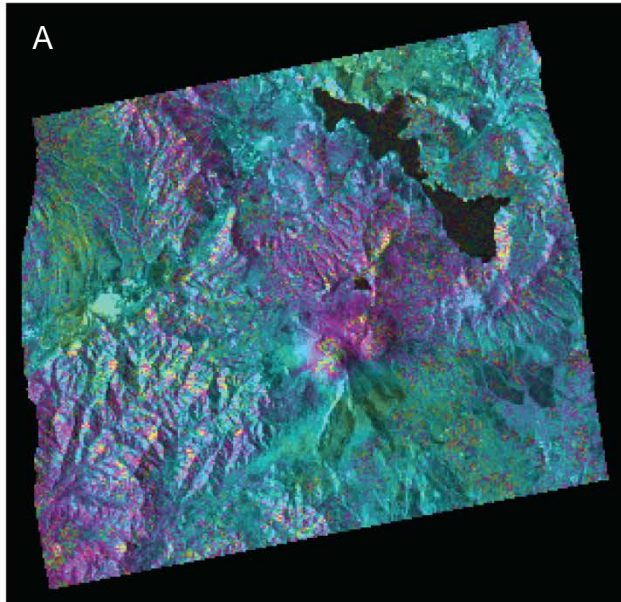
2007/02/03-2007/12/22: Bperp = 206 m

B
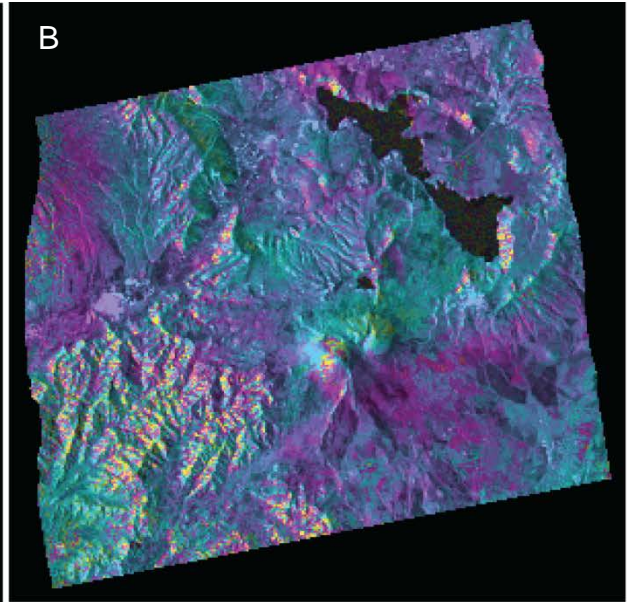
2007/12/22-2008/02/06: Bperp = 522 m

C
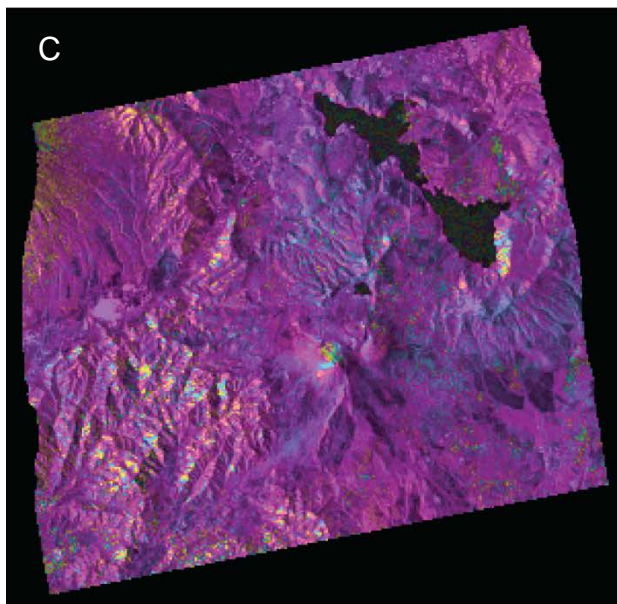
2008/02/06-2008/05/08: Bperp = 209 m

D

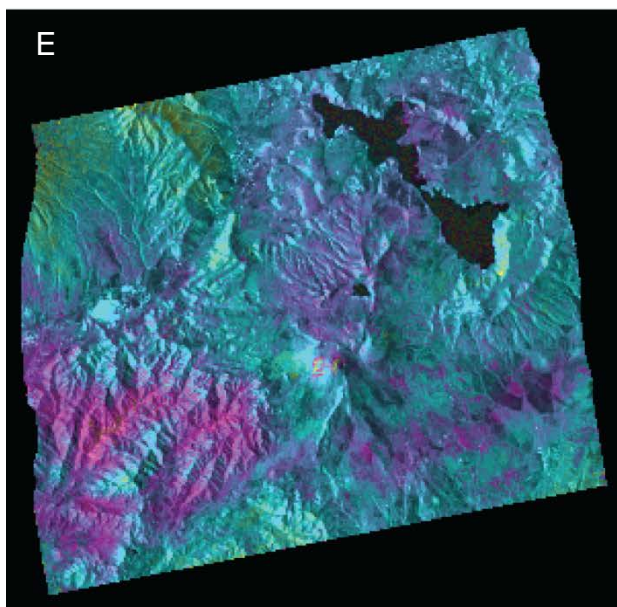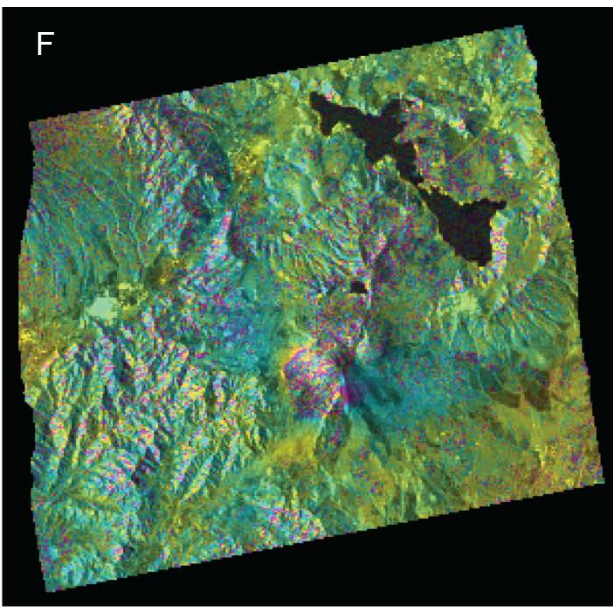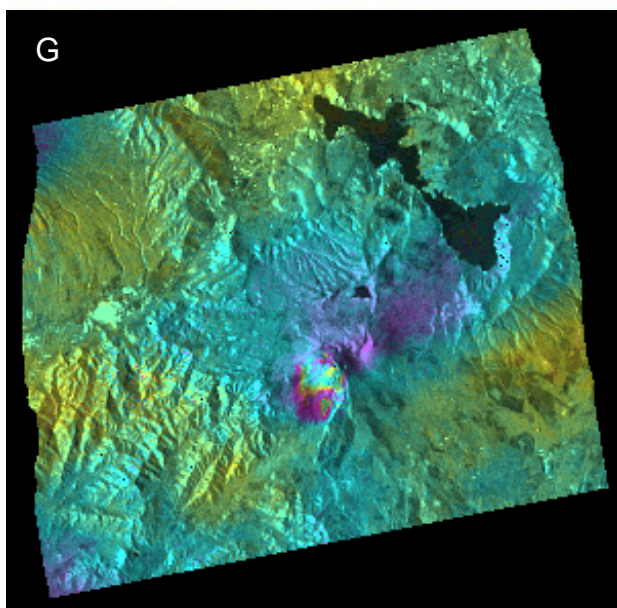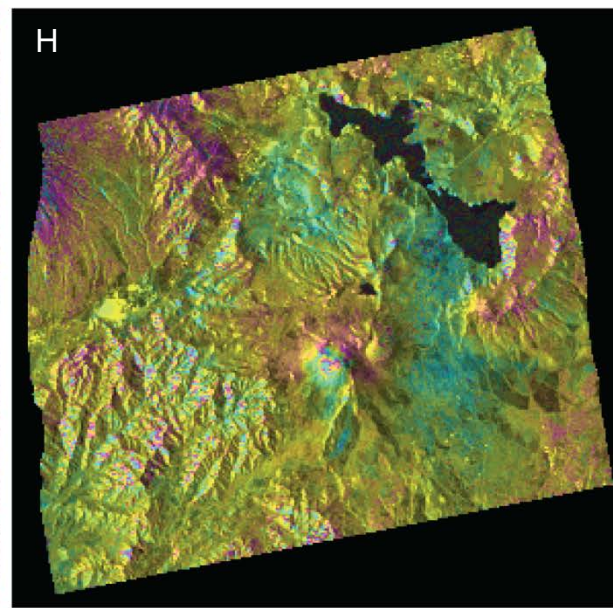2008/05/08-2010/02/11: Bperp = -517 m

N

0 — 11.8 cm

5 km

LOS

E

2010/02/11-2010/03/29: Bperp = -77 m

F

2010/03/29-2010/12/30: Bperp = 369 m

G

2010/05/31-2010/07/16: Bperp = 47 m

H

2010/06/29-2010/08/14: Bperp = 310 m

N

0   11.8
      cm

5 km   LOS

2010/08/14-2010/09/29: Bperp = 116 m

2010/09/29-2010/12/30: Bperp = -171 m

2010/12/30-2011/02/14: Bperp = 421 m

2011/02/14_2011/04/01: Bperp = -77 m
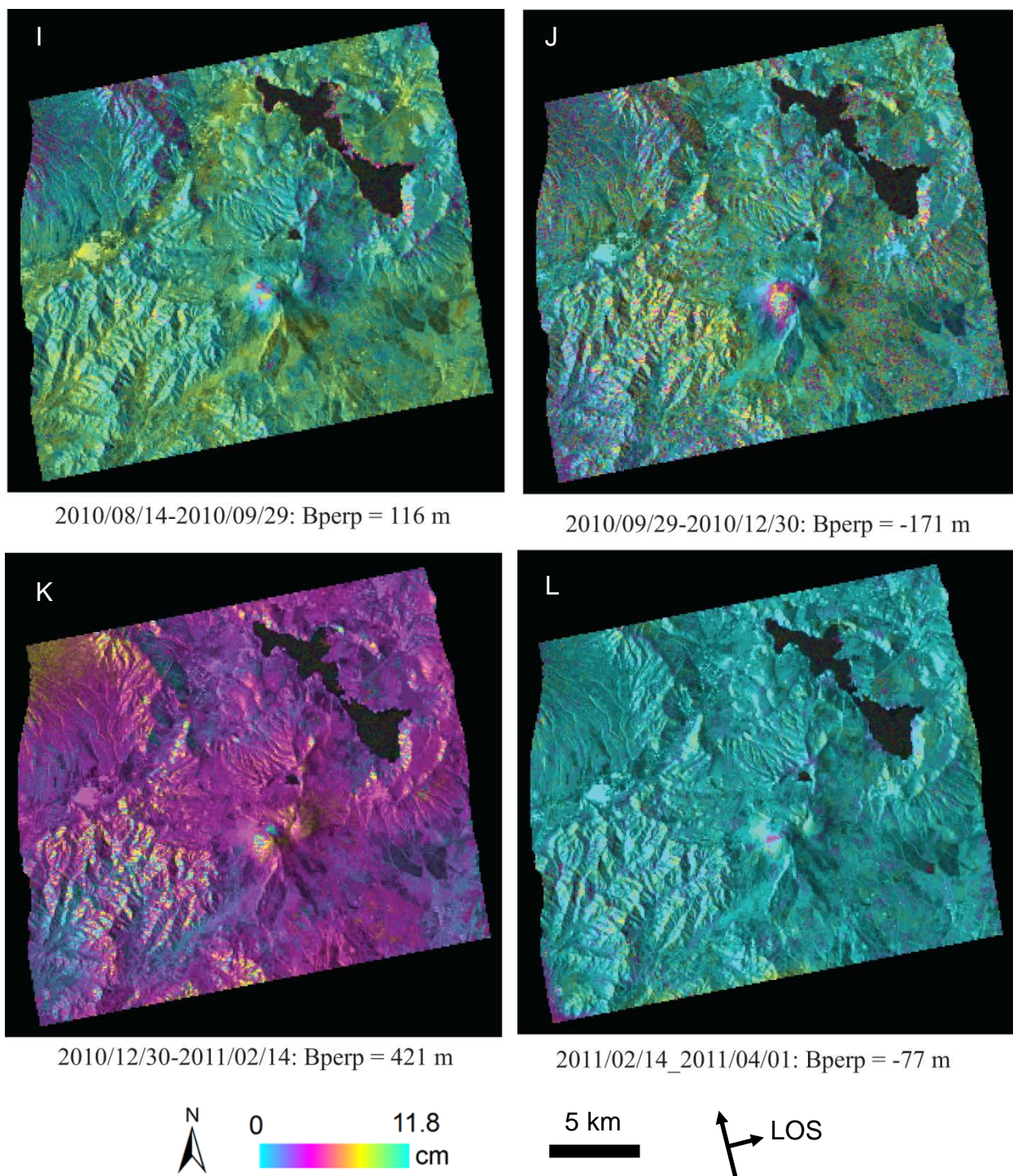
N

0   11.8

cm

5 km   LOS

Figure DR5. ALOS time series interferograms (A-E) before, (F) during, and (G-L) after the May 2010 eruption allow us to constrain edifice deformation related to slope instability to the May 2010 eruption due to the lack of fringes before or after this event.
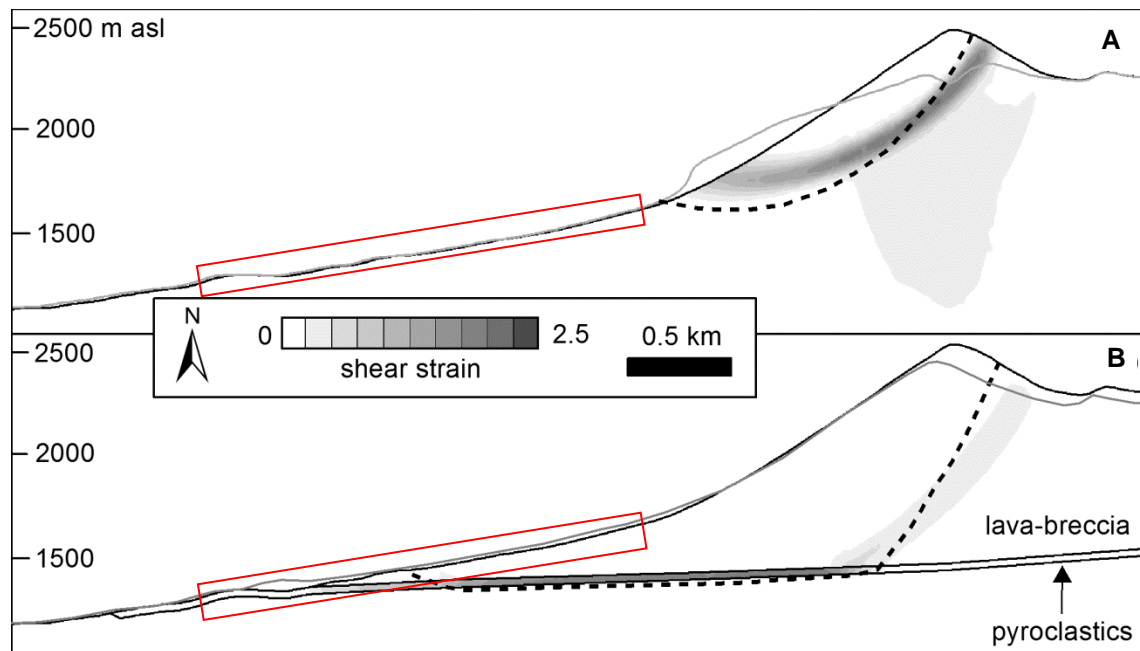
Figure DR6. Numerical modeling results of a 2D cross section of the SW flank of the edifice (A) without a bed of pyroclastics beneath the edifice vs. (B) with pyroclastics. We assume that the tephra layer beneath the edifice in (B) has an aggregated thickness of 30m, similar to the exposed sequences that can be found to the north of the edifice (see Schaefer et al. [2013] for complete discussion on geologic features). Slope stability was modeled using the Hoek-Brown failure criterion (Hoek, 1994) with Limit Equilibrium Methods (LEM) using Rocscience Slide software. Stress-strain variations and deformation were modeled with Finite Element Methods (FEM) using Rocscience Phase2 software. LEM potential failure surface is marked with a black dashed line, and the exaggerated deformed FEM boundary is marked with a solid grey line. The red box shows the area of deformation seen in the coherent regions of the interferograms (see Fig. 2). The volcano's material properties are modeled using a uniaxial compressive strength of 52 MPa, a geological strength index of 50, and a unit weight of 25.65 kN/m^3 after Schaefer et al. (2013). This pyroclastic layer was modeled with a uniaxial compressive strength of 20 MPa, a geological strength index of 15, and a unit weight of 15 kN/m^3. Without the pyroclastic layer (A), the potential failure surface (surface with the lowest ratio of resisting to driving forces) is shallow. Additionally, the shear strain is concentrated in a semi-circle on the upper flank, forming a bulge of deformation centered around 1900 m. With the pyroclastic layer (B), shear strain is concentrated within the pyroclastics, leading to a large potential failure surface that

daylights around 1400 m. The deformation in the latter model more closely mimics the location and style of slope movement measured with InSAR, suggesting that the volcano may be sitting on a weak basement layer.
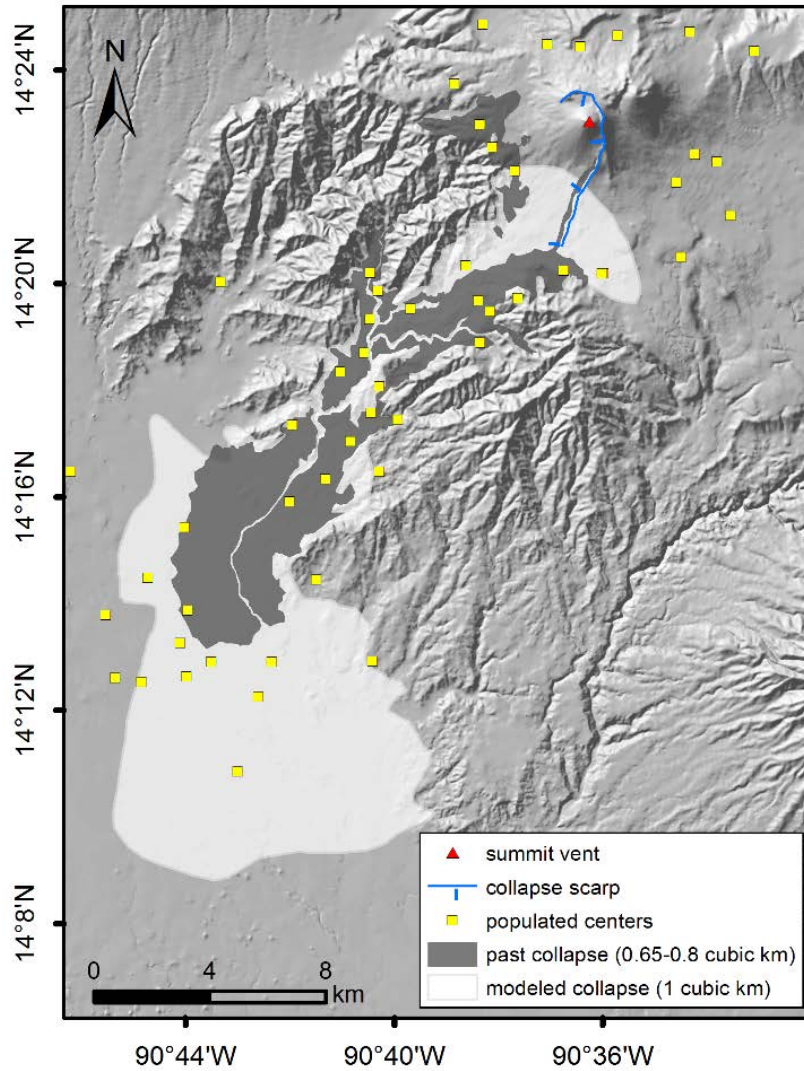
Figure DR7. Debris avalanche hazards associated with sector collapse at Pacaya. InSAR measurements show that the areas of instability extend over the collapse scarp (Fig. 2A and B). This suggests that if a sector collapse were to occur in the future, the resulting debris flow could contain a larger portion of the edifice than the last major collapse. Modeling shows that a debris avalanche containing 1 km^3 of material (in white) could inundate over 100 km^2 more than the ancestral debris avalanche, which contained 0.65-0.8 km^3 of material (in black). Past collapse outlined after: Kitamura and Matias (1995).

References

Hetland, B.R., 2014, A Surface Displacement Analysis for Volcan Pacaya from October 2001 through March 2013 by Means of 3-D Modeling of Precise Position GPS Data [Master's Thesis]: Houghton, Michigan, Michigan Technological University, 84 p.

Kitamura, S., and Matías, O., 1995, Tephra stratigraphic approach to the eruptive history of Pacaya volcano, Guatemala: Science Reports–Tohoku University, Seventh Series: Geography, v. 45, p. 1-41.

Matías Gómez, R.O., Rose, W.I., Palma, J.L., and Escobar-Wolf, R., 2012, Notes on a map of the 1961–2010 eruptions of Volcán de Pacaya, Guatemala. Geological Society of America Digital Map Chart Series, 10, doi:10.1130/2012.DMCH010.

Schaefer, L.N., Oommen, T., Corazzato, C., Tibaldi, A., Escobar-Wolf, R., and Rose, W.I., 2013, An integrated field-numerical approach to assess slope stability hazards at volcanoes: The example of Pacaya, Guatemala: Bulletin of Volcanology, v. 75, doi:10.1007/s00445-013-0720-7.